**PRESSURE CONTROLLER
OF A
CHEMICAL-FREE GAS DEHYDRATION UNIT**

By

KHAIRIL ANUAR BIN MOKHTAR

DISSERTATION

Submitted to the Electrical & Electronics Engineering Programme
in Partial Fulfillment of the Requirements
for the Degree
Bachelor of Engineering (Hons)
(Electrical & Electronics Engineering)

Universiti Teknologi Petronas

Bandar Seri Iskandar

31750 Tronoh

Perak Darul Ridzuan

CERTIFICATION OF APPROVAL

**Pressure Controller
Of a
Chemical-Free Gas Dehydration Unit**

by

Khairil Anuar bin Mokhtar

A project dissertation submitted to the
Electrical & Electronics Engineering Programme
Universiti Teknologi PETRONAS
in partial fulfilment of the requirement for the
Bachelor of Engineering (Hons)
(Electrical & Electronics Engineering)

Approved:

_____

Pn. Noor Hazrin Hany Mohamad Hanif
Project Supervisor

UNIVERSITI TEKNOLOGI PETRONAS

TRONOH, PERAK

December 2009

CERTIFICATION OF ORIGINALITY

This is to certify that I am responsible for the work submitted in this project, that the original work is my own except as specified in the references and acknowledgements, and that the original work contained herein have not been undertaken or done by unspecified sources or persons.

_____

Khairil Anuar bin Mokhtar

ABSTRACT

The purpose of this Final Year Project entitled "Pressure Controller of a Chemical-free Gas Dehydration Unit" is to design and analyze a pressure controller for an alternative method of gas dehydration. Physical separation of water vapor from natural gas is used as an alternative to the conventional method of using chemicals such as Glycol. Dewpoint of water vapor and temperature to condense the condensates are the major concern to allow a physical separation. Research on fluid dynamics determines the conditions that allow water vapor to reach its dewpoint. Pressure, velocity, and temperature of raw natural gas are the main parameters that need to be controlled for this process. The existing system implements a PID controller to control the inlet/outlet pressure ratio as it has causal relationships with velocity and temperature. However, the main problem with this paradigm is the stability of the system. Pressure fluctuation causes the valve to oscillate, thus reducing its efficiency. A Neural Network Controller on the other hand was proven to be a better option in terms of controlling such non-linear properties. Therefore, it has been selected to control the process in this research. From previous findings, it is estimated that the supersonic separator is able to recover around 15 to 20 bbl/MMscf more NGL compared to conventional TEG separator. Based on these facts, it is proven that a Neural Network Controller would be able to further increase the efficiency of the system, thus increasing the production rate of any natural gas recovery operation.

ACKNOWLEDGEMENTS

TABLE OF CONTENTS

LIST OF TABLES

LIST OF FIGURES

LIST OF ABBREVIATIONS

CFD	Computational Fluid Dynamics
FYP	Final Year Project
JT	Joule Thomson
LPG	Liquid Petroleum Gas
LTS	Low Temperature Separator
NGL	Natural Gas Liquids
NMPC	Non-Linear Model Predictive Controller
PID	Proportional Integral Derivative
TEG	Triethylene Glycol
SISO	Single Input Single Output

CHAPTER 1

INTRODUCTION

1.1 Background of Study

Natural Gas has been discovered centuries ago. Since then, gas processing industries have been trying to figure out a way to separate water vapour from raw natural gas for gas transportation purposes such as in export gas pipelines. Chemicals have been used in early stages to absorb water vapours and still being used until today. However, this process requires the chemicals to be treated properly to avoid accidental pollution. Throughout the years, further understanding on physics, lead scientist to the discovery of gas behaviour in high speed compressible flow[1]. This knowledge was then applied in aerospace engineering for designs of high-thrust rockets and engines. Along with that, came the gas centrifuge technology that is used in Uranium Enrichment process[2]. These two technologies were then combined in order to come out with a physical separation process in gas processing industries that does not require any involvement of chemicals. This concept was first introduced by Twister BV, a company formed by Shell and two other major oil and gas company. A first commercialized package was implemented in 2004 on Shell Sarawak's B-11 offshore platform[3].

1.2   Problem Statement

Water vapour in natural gas is a major problem in gas processing industries. It results in corrosion and blockage inside pipelines, valves and other process equipments. A conventional dehydration unit uses chemicals such as Triethylene Glycol (TEG) to absorb water from raw natural gas. However, these chemicals need to be managed properly and any accidental disposal would cause a severe pollution. Apart from that, a conventional gas dehydration unit requires a large space. A physical separator is better for dehydration purposes as it is economic, eco-friendly, and more efficient. The pressure controller of this type of separator needs to maintain the conditions that will allow physical separation and to ensure the safety of the process.

A compressible flow that consists of a shockwave is highly irreversible and cannot be assumed to be isentropic. Since physical separators involve a method of controlling the position of shockwave, it is important that the controller must be able to handle the characteristic of pressure and velocity distribution throughout the separator. This process needs to be modelled and a controller needs to be built based on this model.

1.3   Objectives and Scope of Study

The main objectives of this project are:

1.   To design a physical system of a supersonic separator.
2.   To model the characteristic and behaviour of a compressible flow in a supersonic separator.
3.   To design a controller for a supersonic separator based on its behaviour and characteristic model.

The scopes of study in this project are:

1. Research on dewpoint of water vapour and temperature for condensate to condense. Also the water content and composition of raw natural gas.
2. Conditions of fluid dynamics that enable physical separation based on process conditions.
3. Design, simulation and analysis of a pressure controller that operates on fluid dynamics condition.

CHAPTER 2
LITERATURE REVIEW

2.1   Supersonic Separator

A chemical-free gas dehydration unit uses the same concept as a turbo-expander where highly pressurized gas is expanded using a 'De Laval Nozzle' (or convergent-divergent nozzle) to a supersonic speed. This expansion will cause the velocity to increase which in turns, cause the temperature and pressure to decrease rapidly [1]. This temperature drop will provide a suitable condition for water and condensates formation. A guide vane will then centrifuge the condensed water and natural gas liquids (NGL) to separate it from raw natural gas with the same Gas Centrifuge concept as used in Uranium enrichment. A cone shaped tube at the centre of this vortex is used to collect natural gas (methane) from this separation.

From a study of NGL recovery [4], a comparison of Twister's performance has been made with a Joule-Thomson Low Temperature Separator (JT-LTS) system through a series of simulations where three simulation parameters were studied. The parameters are Feed Pressure (100 bara, 70 bara, and 40 bara), Pressure Loss (25%, 35%, and 45%), and Feed Water Content (7lb/MMscf, 5lb/MMscf, 3lb/MMscf, and 1lb/MMscf). For every parameters, three feed gas composition were studied; Lean, Normal, and Rich. Results show that with a feed pressure of 100bar, and downstream pressure of 55bar to 75bar, the improvement is typically around 0.8 to 1.0 tonnes/MMscf more Liquid Petroleum Gas (LPG) and 15 to 20 bbl/MMscf greater NGL recovery. This shows that the Twister system produces a higher production rate than any other separation system available today.

2.2 Gas Behaviour

A De Laval Nozzle (or convergent-divergent nozzle) is an hourglass-shape tube that is pinched in the middle. It is used as a means of accelerating the flow of a gas passing through it to a supersonic speed. The different properties of gas traveling at sonic and subsonic speed are the main operating principle of a De Laval Nozzle [1].

From a study [5], it shows that for a compressible supersonic flow, an increase in cross-sectional area will result in the acceleration of gas passing through it. This is due to the constant mass flow rate of the gas. Apart from that, a significant change in velocity results in changes of pressure and temperature as shown by [6],[7]. This changes can be described as a normalized parameters of gas flow in *Appendix A* where p_0 is the feed pressure, T_0 is the feed temperature, $A*$ is the area at sonic throat, Ma is the local mach number, A is the local area, p is the pressure local pressure, and T is the local temperature.

This behavior of gas is used in this study to determine the geometry of the physical system that is simulated.

2.2.1 *Shockwave*

For every supersonic compressible flow, the formation of shockwave is almost inevitable. There are two types of shockwave namely; Normal Shock and Oblique Shock. However for a supersonic flow in a convergence-divergence nozzle (also sometimes referred as expansion tube), only normal shock would appear in the tube as shown by studies in [5],[8],[9].

A normal shockwave is a shockwave that occurs in a plane normal to the direction of flow. The flow process is highly irreversible and cannot be approximated as being isentropic [7].

For a swirling flow [5], at the instant of the beginning of swirling, a large toroidal vortex arises in the separator part behind the extraction cone. The non-uniformity of angular components of gas velocity in the tube increases, thus involves a redistribution of pressure in the tube which corresponds to the emergence of return

5

flows. This non-uniformity is shown in *Figure 1* and *Figure 2* where r is the radius from the centre of the tube. With further development of swirling flow, the toroidal vortex penetrates deeper into the supersonic zone of the tube, and therefore causes the emergence of shockwave. It was suggested that the presence of shockwave prevents the gas from expanding to such extend that the temperature in the region of extraction would turn out to be low enough for the condensation of components of interest [5].
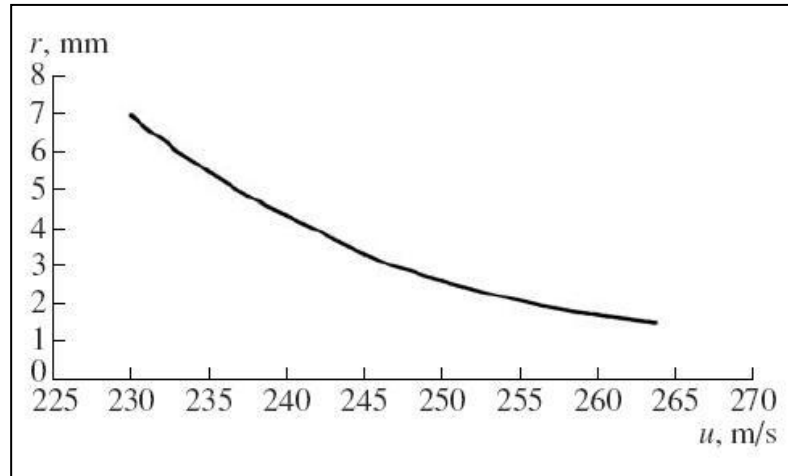
Figure 1   :The longitudinal component of velocity *u*.
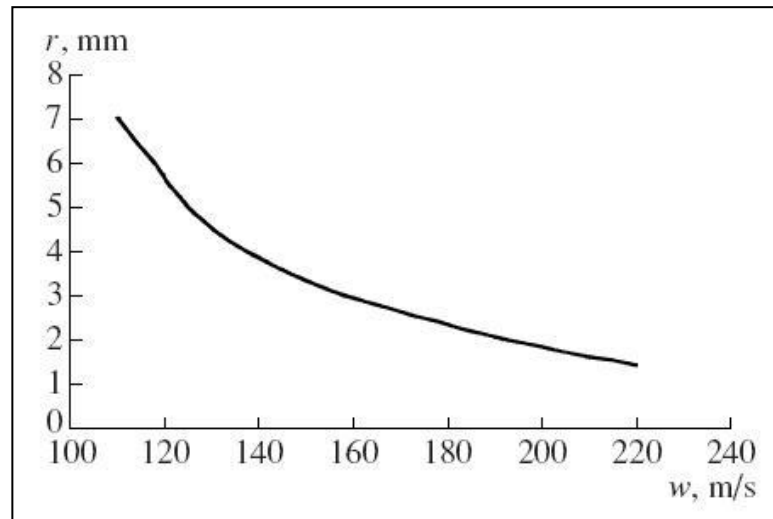
Figure 2   :The tangential component of velocity *v*.

Therefore, in this research, the position of shockwave is varied by the manipulation of flow velocity.

2.3   Neural Network

Neural networks nowadays are being used in a wide area of industries. Even though it has been discovered for decades, not until recently it is being widely applied due to the rapid development in computing power that enables neural networks to be trained in short time durations when modelling the behaviour of complex systems [10].

In an article [11], a research [12] was reviewed on a new kind of spiral tube compound gas-liquid separator. The design of the structure of the spiral tube was validated by numerical simulations. Three control plans were compared before the plan to keep liquid level stable by controlling gas exit out flux was chosen. The proposed method was proven to be feasible by automatic and manual experiments. By manual experience and Ziegler-Nichols step response method, a Fuzzy-PID controller was designed. Experiments on this controller indicated that the controller has excellent anti-jamming performance and three times more efficient compared to a gravity separator in practical separation.

However, in this research, a different method has been chosen. The whole process is controlled by a Neural Network Controller with Lavenberg-Marquardt algorithm, without functions of a PID algorithm.

CHAPTER 3
METHODOLOGY

3.1   Procedure Identification

In order to achieve the objectives of the project, research and investigation were done on the dewpoint at a given constant barometric pressure. This was to determine the operating conditions that were needed for a physical separation. Part of the research has also involved in determining the temperature that causes the formation of natural gas liquids (NGL).

Analysis on fluid dynamics was made to determine the main control variable based on water dewpoint and NGL formation temperature. Dimension and sizing of the gas dehydration unit were also determined from this analysis. The operating region of the process was defined by the maximum and minimum pressure that allows physical separation.

Based on the variables that were determined in fluid dynamics analysis, a Neural Network pressure controller was built using Matlab. The controller controls the variables in order for the physical separation to be possible. This involves the control valves reaction to control the pressure ratio due to increasing or decreasing of feed gas pressure. Simulation and analysis of the system using Matlab were made to analyze and characterize the controllability and stability of the system.

Flow Chart of procedures is represented in *Figure 3* and steps are further elaborated.

START

Identification of operating region from production

Geometry dimensions calculation

Gambit 2.2.30

Physical system drawing

Define boundary conditions

Volume mesh

Fluent 6.2.16

Define parameters and initial conditions

CFD Simulation

Gas Behavior

Identification of process function, specification and

Selection of controller type/paradigm and control

Compressible Flow analysis

Input/Output

Matlab R2008a

Data arrangement

System construction and parameters

Neural Network system training

Analysis of performance

Acceptable performance?   No

Yes

Performance

Analysis of results and discussion

Conclusion

FINISH

Figure 3   **:**Project Flow Chart.

3.2 Research

3.2.1 Identification of Operating Region

Since the system is designed to a specific active well, Shell B-11 platform was selected as it is an active gas producing platform. The specifications are as stated in *Table 1* below:

Table 1 **:**Shell B-11 Production Specifications [17].

Fact sheet on B11	
PSC	MLNG-Dua (21 May 1995 - 20 May 2015)
PSC Partners	Sarawak Shell Berhad (50% equity, Operator) PETRONAS Carigali Sdn. Bhd. (50% equity)
Location	170 km north of Bintulu and 65 km east of E11, in a water depth of 300 ft
Discovery	1980 (by exploration well B11-1)
Appraisal	1992(byB11-2)
Reservoir Type	Unfaulted platform type carbonate buildup of Miocene age
Gas Water Contact	10,271 ft ss
Areal Extent at GWC	7x4 square km
Expectation Hydrocarbon In-Place Volume	Gas: 1.90 Tscf NGL: 41.8 MMb
Reserves Volume	Gas: 1.62 Tscf NGL: 26.9 MMb
Gas column	1070 ft
Initial Reservoir Pressure @ 9,850 ft ss	4,484 psia
Condensate Gas Ratio	21-23 b/MMscf
Gross Heating Value	874 - 997 Btu/scf

Contaminants	CO2: 7-18% H2S: 280-1,700 ppm
Supply Route	Via E11R-B to the MLNG plant in Bintulu
Wells	5 sub-horizontal wells and 1 water disposal well
Platform capacity	600 MMscf/d

3.3 Experimental Works and Simulations

3.3.1 Geometry Dimensions Calculation
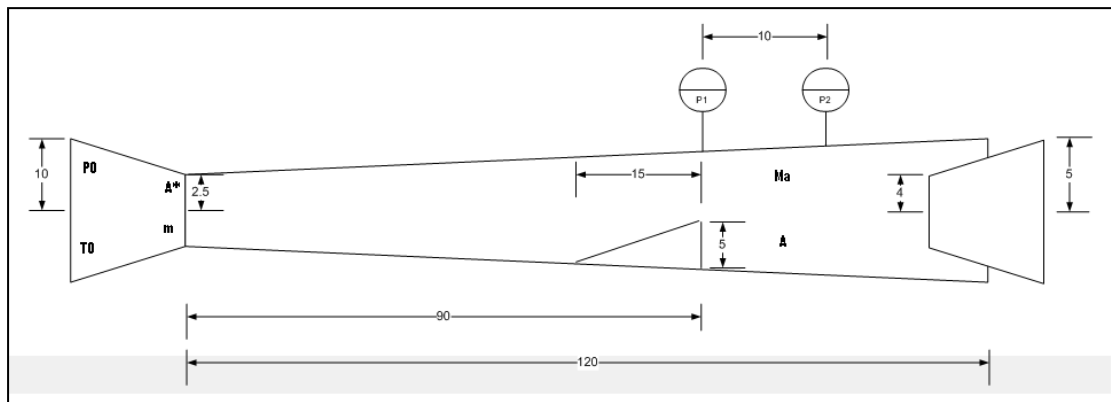
Figure 4   :Geometry Calculation.

Based on the production specifications, dimensions of the physical system were calculated (in cm). For the following equations, R is the gas constant (287 $m^2/(s^2.K)$), A is the local area, A* is the throat area, P0 is the inlet pressure, m is the mass flow rate, and T0 is the inlet temperature. The relationship between mass flow rate and area ratio is defined by the following equation:

$$A* = \frac{m}{0.6847} \frac{\sqrt{RT0}}{P0}$$ (Eq. 1)

The desired Mach Number, Ma is related to the area ratio, A/A* by the following equations:

$$Ma\ (Subsonic) = \begin{cases} \dfrac{1+0.27[\frac{A}{A*}]^{-2}}{1.728[\frac{A}{A*}]} & for\ 1.34 \leq \frac{A}{A*} \leq \infty \\[3mm] 1 - 0.88[\ln\frac{A}{A*}]^{0.45} & for\ 1.0 \leq \frac{A}{A*} \leq 1.34 \end{cases}$$ (Eq. 2)

$$Ma\ (Supersonic) = \begin{cases} 1 + 1.2[\frac{A}{A*} - 1]^{0.5} & for\ 1.0 \leq \frac{A}{A*} \leq 2.9 \\[3mm] [216[\frac{A}{A*}] - 254[\frac{A}{A*}]^{\frac{2}{3}}]^{\frac{1}{5}} & for\ 2.9 \leq \frac{A}{A*} \leq \infty \end{cases}$$ (Eq. 3)

The dimensions of physical system were then determined by the area ratio.

3.3.2   Physical System Drawing

From calculated geometry dimensions, the physical system was then drawn in Gambit 2.2.30 as shown in *Figure 5* below.
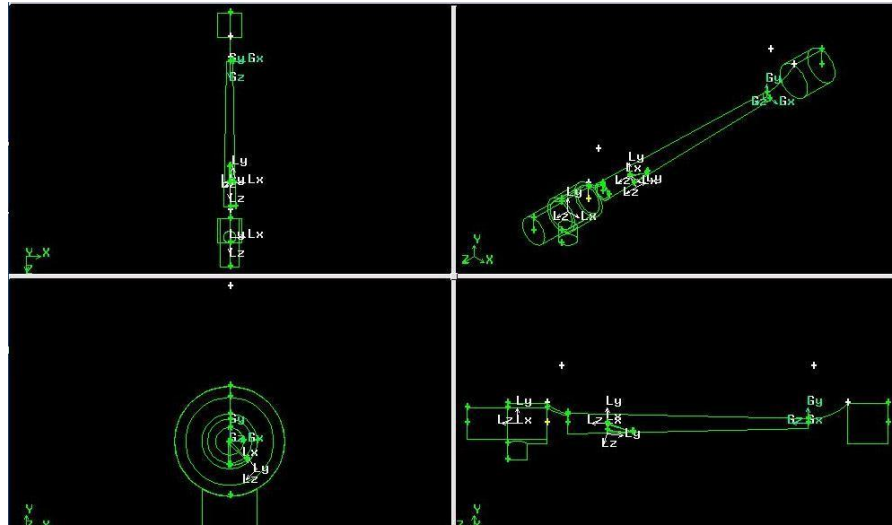
Figure 5   **:**Physical System Drawing.

3.3.3   Define Boundary Conditions

From the physical system drawing, the boundary conditions were then defined. Volumes were defined as fluid while surfaces were defined as solid as shown in *Figure 6* below.
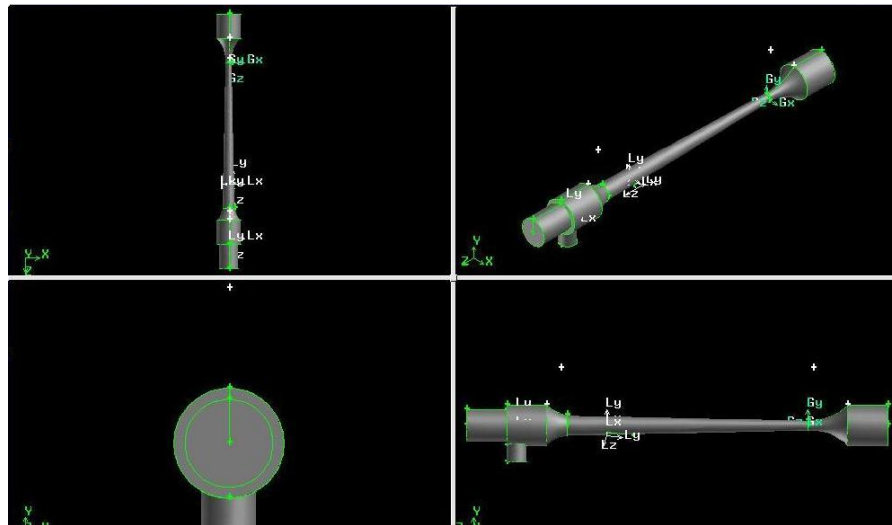
Figure 6   **:**Defined Boundary Conditions.

The physical system was then meshed and the results are in a form of volume meshes. This result is shown and further discussed in Chapter 4 (*Figure 11*).

3.3.4   Define Parameters and Initial Conditions

Volume meshes from Gambit 2.2.30 were then imported into Fluent 6.2.16 for simulations. Parameters were defined and initial conditions were set.

3.3.5   CFD Simulation

The volume meshes were then simulated and behaviour if the flow was observed. Results were in a form of pressure distribution along the duct. This result is further discussed in Chapter 4 (*Figure 12*).

3.3.6   Identification of Function, Specification and Variable

The results from CFD Simulation were then analyzed to determine the characteristic of a supersonic compressible flow. From this analysis, pressure has been identified to be the main process variable (input) while output valve percentage is the control variable (output) since its manipulation varies the flow velocity which has a causal effect on the flow pressure.

3.3.7   Selection of Controller Type and Control Strategies

Since the pressure across a shockwave fluctuates rapidly, a conventional single-input-single-output (SISO) system with a PID algorithm will not be able to determine the exact position of shockwave due to its dual-profile (supersonic and subsonic) characteristic. A pressure ratio PID algorithm system on the other hand will swing out of stability as the feedback system tries to make the necessary corrective action. This is due to the rapid changes of pressure. Therefore, a Neural Network Controller was selected due to its predictive characteristic that enables it to predict the position of shockwave based on a feedforward back propagation system. In this case, the 3 inputs are feedforwarded into the system. The correlation between inputs and output is constantly evaluated and back propagated inside the controller. Valve

percentage opening is then predicted based on this correlation and not directly from the input. This control strategy is graphically described in *Figure 7*.
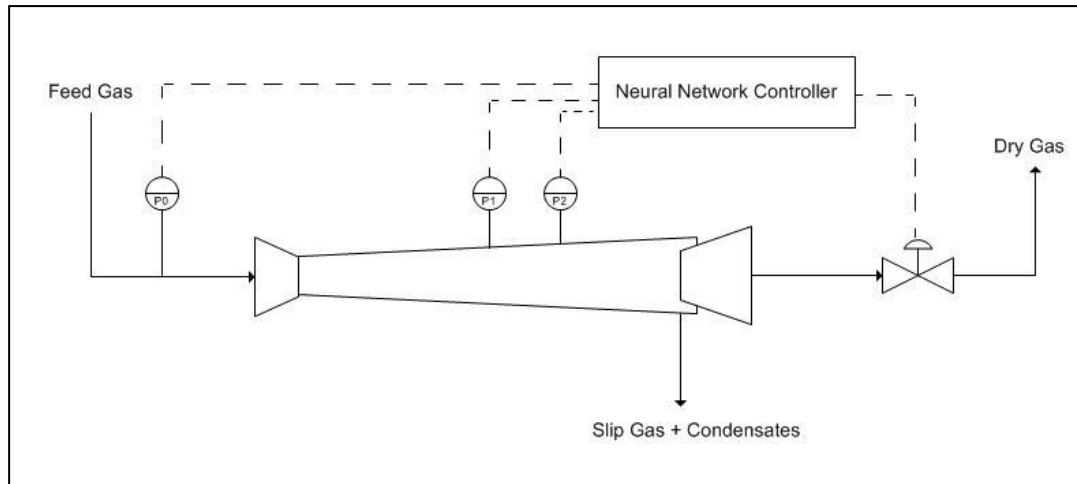
Figure 7   :Control Strategy

3.3.8   *Compressible Flow Analysis*

Area Ratio

In this part of the analysis, there are three major variables that were analyzed, namely, Area, Mach Number, and Pressure. Based on the analysis of fluid mechanics, these variables were calculated based on the ratio of Local Area with Critical/Sonic Throat Area.

Mach Number

The local Mach Number profile is defined by the following equation:

$$Ma\ (Subsonic) = \begin{cases} \dfrac{1+0.27[\frac{A}{A_*}]^{-2}}{1.728[\frac{A}{A_*}]} & for\ 1.34 \le \dfrac{A}{A_*} \le \infty \\ 1 - 0.88[\ln\frac{A}{A_*}]^{0.45} & for\ 1.0 \le \dfrac{A}{A_*} \le 1.34 \end{cases} \quad \text{(Eq. 4)}$$

15

$$Ma\ (Supersonic) = \begin{cases} 1 + 1.2[\frac{A}{A*} - 1]^{0.5} & for\ 1.0 \le \frac{A}{A*} \le 2.9 \\ [216[\frac{A}{A*}] - 254[\frac{A}{A*}]^{\frac{2}{3}}]^{\frac{1}{3}} & for\ 2.9 \le \frac{A}{A*} \le \infty \end{cases} \qquad \text{(Eq. 5)}$$

where Ma is the Mach Number, A is the Local Area, and A* is the Sonic Throat Area.

Velocity

For a compressible flow, Velocity is related to Mach Number by the following equation:

$$V = Ma\ x\ \alpha \qquad \text{(Eq. 6)}$$

where Ma is the Mach Number and α is the speed of sound.

Pressure

Pressure of a compressible flow is described by:

$$\frac{P1}{P0} = \frac{1}{(1+0.2Ma^2)^{3.5}} \qquad \text{(Eq. 7)}$$

where P1 is the local pressure, P0 is the inlet pressure, and Ma is the Local Mach Number. The overall function for the upstream profile is attached in *Appendix B*.

Downstream Profile

When a normal shockwave occur in a compressible flow of a duct, there are two pressure profiles that need to be considered. The upstream section of the shockwave would have the profile of a supersonic flow while the downstream section would have the profile of a subsonic flow as shown in *Figure 8* where Ma_1 is the supersonic Mach Number while Ma_2 is the subsonic Mach Number. This behavior was carefully considered in designing the system as shown in *Figure 9*.
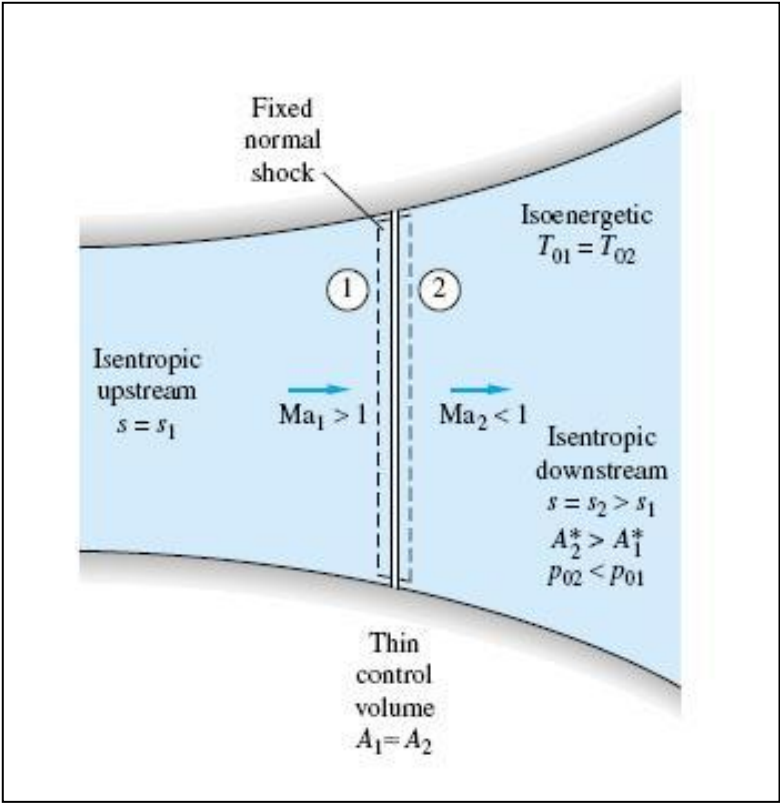
Figure 8   :Flow Characteristic Across a Shockwave [3].
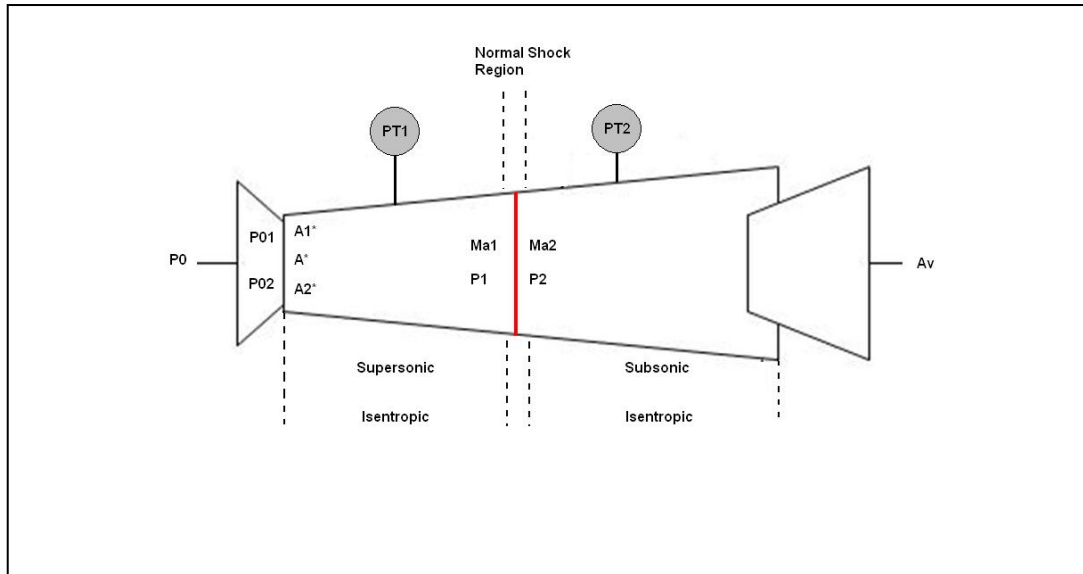
Figure 9   :Implementation of Flow Characteristic Across a Shockwave.

Since the shockwave is positioned in between Pressure Transmitter 1 (PT1) and Pressure Transmitter 2 (PT2), the control zone is between 0.95m to 1m from the sonic throat. The corresponding radius is between 0.0448m to 0.0458m. From this specified range, the concerning Pressure Profile was determined from its Mach Number and Operating Range of 50bar to 150bar in Matlab.

Pressure Relation

For a perfect gas all the property ratios across the normal shock are unique functions of specific heat ratio, *k* and upstream Mach Number, Ma$_1$. Thus, for a given upstream mach number and upstream pressure, P1 the downstream pressure, P2 is given by:

$$P2 = P1 \frac{1}{2.4}[2.8Ma_1^2 - 0.4] \hspace{3cm} \text{(Eq. 8)}$$

Mach Number Relation

Relating the mach numbers between the upstream and downstream side of a shockwave, results in the following equation:

$$Ma_2 = \left[\frac{0.4Ma_1^2 + 2}{2.8Ma_1^2 - 0.4}\right]^{\frac{1}{2}}$$ (Eq. 9)

Effective Area Relation

For every change in the position of shockwave, the downstream Mach number would also change. This in turn would change the effective area at any given point on the downstream side. The effective area relation is given by:

$$A_2^* = A_1^* \left[\frac{Ma_2}{Ma_1}\right]\left[\frac{2 + 0.4Ma_1^2}{2 + 0.4Ma_2^2}\right]^{0.48}$$ (Eq. 10)

Valve Area

The mass flow rate at any given valve area, A_v is equal to the mass flow rate at a point in the duct which have the same area. Thus, from the corresponding downstream effective area, the area at which a normal shockwave would occur is calculated by the following equation:

$$A_v = A_2^* \frac{[1 + 0.2Ma_1^2]^3}{1.728Ma_1}$$ (Eq. 11)

The overall function of downstream profile is attached in *Appendix C* and results are further discussed in Chapter 4 (*Table 2*).

3.3.9   Data Arrangement

From the results of input/output correlation in Compressible Flow Analysis, the data were then imported into Matlab for Neural Network System construction. Before the data can be used, it needs to be pre-processed. This was done by randomizing it to ensure that the system covers the whole range of data. After it has been randomized, the data was divided into two for training and validation purposes.

3.3.10   System Construction and Parameters Initialization

The system was constructed in Matlab where the goal is to reach a mean squared error (mse) of 0.001 at most with 10000 maximum number of iterations. The network architecture is graphically described in *Figure 10*.
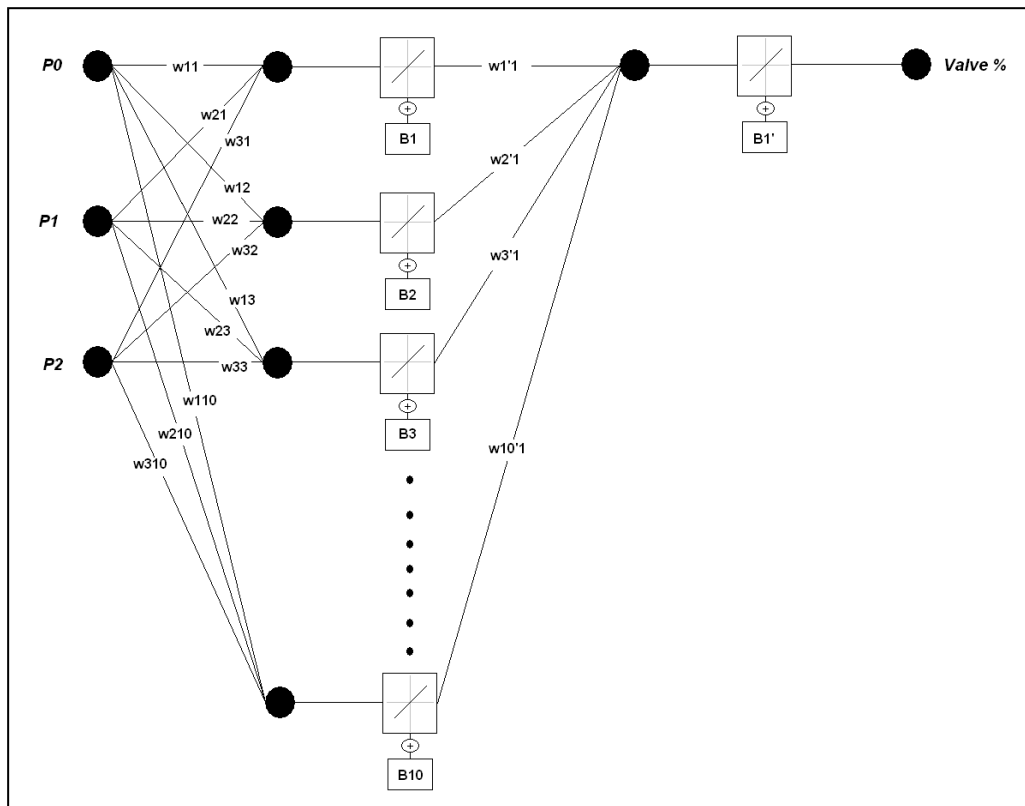
Figure 10   : Neural Network Architecture

3.3.11 *Neural Network System Training*

The data was then trained in neural network by 11 different algorithms. Results from this training are further discussed in Chapter 4 (*Table 3* and *Figure 13*). Matlab Function for this system is attached in *Appendix D*.

CHAPTER 4
RESULTS AND DISCUSSION

4.1   Volume Mesh

From the calculated dimension for physical system geometry, a drawing was made in Gambit 2.2.30. The boundary condition was then defined and volumes were meshed (*Figure 11*).
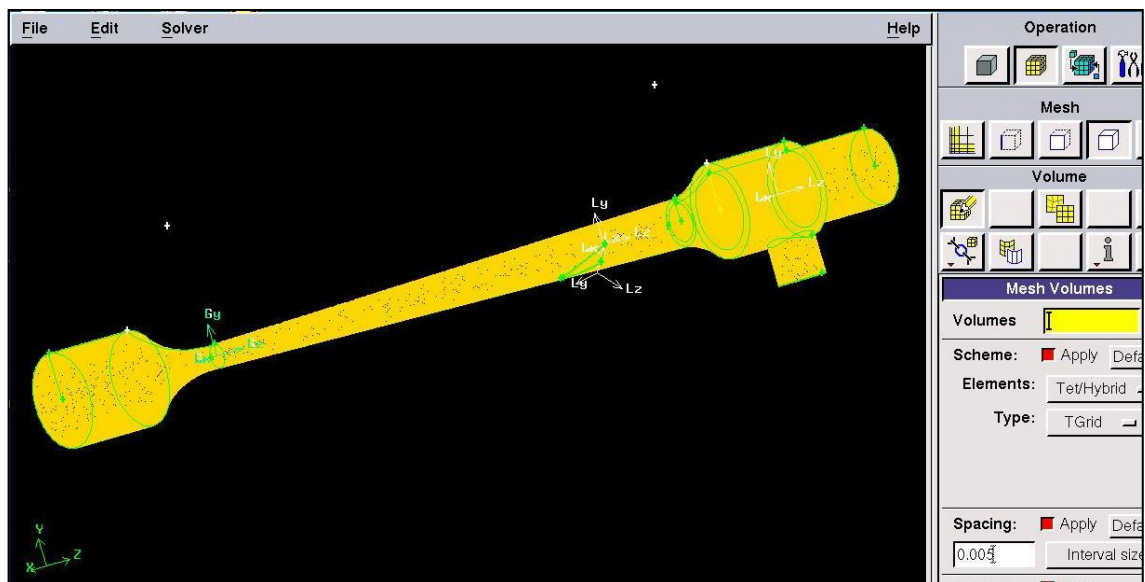
Figure 11   **:**Meshed Volumes in Gambit

4.2   Gas Behaviour

From volume mesh in Gambit, the data was imported into fluent for simulation of grid analysis. These nodes are shown in *Figure 12*.
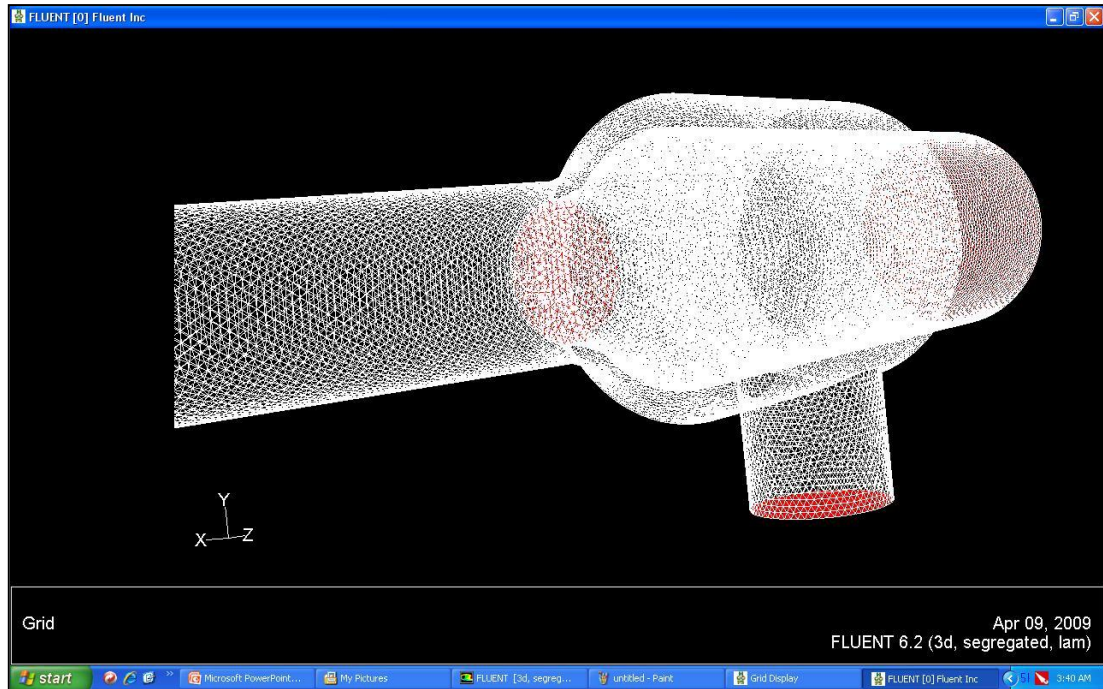
Figure 12   **:**Grid Analysis in Fluent

Based on this analysis, the position of shockwave is identified. It moves back and forth for more than 500Hz. This in turns, results in a high rate of pressure fluctuations. Though in a static condition this pressure relation is linear, the fluctuations in a dynamic condition will cause the system to swing out of stability and its linearity. Thus, a neural network based controller is selected to control the position of shockwave due to its predictive and adaptive characteristic.

In terms of implementation, a pressure transmitter cannot be placed directly at the point of desired shockwave since the fluctuations will cause inaccurate readings due to the fluctuations. A single pressure transmitter of a SISO system on the other hand would not be able to determine whether a shockwave is present due to the dual-profile (supersonic and subsonic) characteristic of a shockwave. Therefore, a dual-transmitter measuring technique was proposed in this research to measure the pressure both upstream and downstream of the shockwave. These inputs are fed into the system together with the feed pressure.

23

Apart from that, the size of transmitter will affect the compressible flow. Obstruction introduced by the tip of transmitters will cause turbulence to occur, interrupting the flow and reducing the efficiency of the process. Smaller transmitter and pressure cells were proposed as means of measurement to provide smaller obstruction in the flow.

4.3   Input / Output

After the control strategy has been determined, calculations were made at desired measuring points to produce an input/output relationship. This data was then used in Matlab for system construction and training. Fraction of this data is shown in *Table 2* below while the whole data is tabulated in *Appendix E*.

Table 2   **:**Control Zone Pressure Profile

Input			Output
P0 (kPa)	PT1 (kPa)	PT2 (kPa)	Valve Opening (%)
106391.25	4642.57560	19126.69	68.03825
112673.40	4916.70864	34046.93	69.09551
108316.42	4726.58411	24074.91	68.39023
113990.62	4974.18815	18146.72	67.68671
111356.17	4859.22913	12825.34	67.3356
106897.87	4664.68310	15157.85	67.68671
115713.15	5049.35365	18872.59	67.68671
106391.25	4642.57560	6463.745	66.98492
115713.15	5049.35365	39320.35	69.44882
112876.05	4925.55164	30073.37	68.74265
106391.25	4642.57560	35480.15	69.44882

4.4 Neural Network Simulation

From the compressible flow analysis, the input/output data was imported into Matlab for system construction and training. The system was trained with 11 different algorithms and the results are shown in *Table 3* below. The source code for Neural Network is attached in *Appendix E*.

Table 3   **:**Results from Controller Simulation

Training Algorithm	Mean Square Error	Epoch	Remarks
Trainbfg	0.000378	9	Target reached
Trainbr	1.08	10000	Max epoch reached
Traincgb	0.000256	5	Target reached
Traincgf	0.000539	12	Target reached
Traincgp	0.000965	10	Target reached
Traingd	0.000995	968	Target reached
Traingdm	0.191	7	Validation failed
Traingda	0.138	25	Validation failed
Traingdx	0.146	12	Validation failed
Trainlm	0.000188	2	Target reached
Trainoss	0.000505	9	Target reached

Trainrp	0.00268	12	Target reached
Trainscg	0.000325	7	Target reached

Based on *Table 3*, the Levenberg-Marquardt (trainlm) algorithm has been identified to give the least error and fastest learning rate. This is shown graphically in *Figure 13* below.
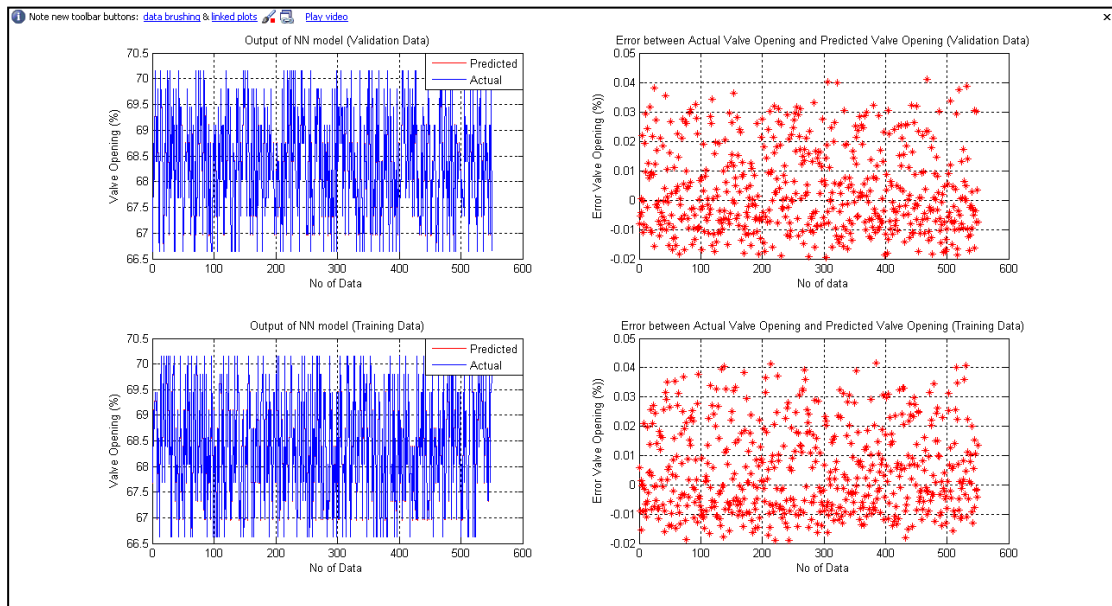
Figure 13   **:**Actual versus Predicted Output

However, this comes with the expense of high memory usage. For a more complex system with more hidden layer and neuron, computational power would be a limiting factor. Therefore, it is suggested by the result from this research that a Gradient Descent (traingd) method is to be used in a more complicated system. Though the learning rate is much slower, the memory usage is much more efficient, making a much complex system training possible.

From this result, it has been proven that a Neural Network Controller is able to handle the non-linear properties of a high fluctuating compressible flow and further increasing the efficiency of the system.

The feedforward system architecture allows for a compensation action to be made at an instance a disturbance is sensed, before the process is interrupted. A feedback system on the other hand, makes a corrective action after an interruption is sensed in the process. This means that the proposed Neural Network controller is able to keep the system in the desired operating region and maintain the process at maximum efficiency.

The back propagation paradigm in the controller allows the output to be predicted based on the input/output correlations. Compared to a feedback PID paradigm whereby the output is determined directly by the input. This means that the proposed Neural Network controller is able to reduce the ripples on the output and therefore increasing its stability while maintaining the transmitter's sensitivity.

CHAPTER 5
CONCLUSION AND RECOMMENDATION

5.1 Conclusion

From this research it is concluded that a compressible supersonic flow can be numerically modelled. Computational Fluid Dynamics simulations proved that the behaviour of the flow is non-linear in a dynamic condition. This simulation also helped to validate the physical system design and determine the best control strategy for the process.

Simulation of the control system shows that the proposed Neural Network Controller is able to handle the non-linear properties and further increasing the stability of the system and the efficiency of the process.

As far as this research is concern, the objectives have been met. However, there are still a lot of improvements that can be made. These are further discussed in the Recommendation part.

5.2   Recommendation

Based on the current results, the accuracy of the simulation can be optimized by several improvements in simulation analysis and initial calculations.

The geometry of the physical system is made based on the assumptions that the specific heat ratio is the same of that an ideal gas while in reality this ratio differs from one well to another depending on the composition of the gas. A more accurate model can be made if the calculations are made based on the condition of a specific well.

The simulation in fluent can be improved by reducing the interval size of mesh. This results in greater number of nodes to be analyzed. Therefore, the simulation results will be more precise. However, smaller interval size comes with the expense of higher computation power and memory usage. This is one of the limitations encountered in this research.

In terms of implementation, it is recommended that the pressure transmitters to be used must have a high sampling rate to ensure that it could handle the high pressure fluctuations and further increasing the stability of the system.

Comparison with a feedback PID algorithm and the existing controller can further validate the proposed Neural Network Controller.

REFERENCES

[1] "De Laval Nozzle", 29 January 2009, http://en.wikipedia.org/wiki/Laval_nozzle

[2] "Gas Centrifuge", 26 November 2008,
http://en.wikipedia.org/wiki/Gas_centrifuge

[3] "First Commercial Twister Supersonic Separator Starts Up", 19 February 2004,
http://www.shell.com/home/content/my-
en/news_and_library/press_releases/2004/twistersupersonicseparator_0219.html

[4] Genesis Oil & Gas Consultants Ltd., "Twister NGL Recovery Study", High
Holborn, London: Genesis Oil & Gas Consultants, January 2008.

[5] M.M. Malyshkina, "The Structure of Gasdynamic Flow in a Supersonic Separator
of Natural Gas", Moscow Institute of Physics and Technology, April 2007.

[6] Frank M. White, *Fluid Mechanics*. Kingston: McGraw-Hill Series, Fourth
Edition, November 1998.

[7] Yunus A. Cengel and John M. Cimbala, *Fluid Mechanics Fundamentals and
Applications*. Kingston: McGraw-Hill Series, First Edition, 2006.

[8] Min-Gyoo Lee, Jong-Ho Park and Michio Nishida, , "Unsteady Shock Waves in
Supersonic Nozzles", in *KMSE International Journal*, Vol. 11, 1993, pp. 96-105.

[9] S. Schlamp and T. Rosgen, "Flow in Near-critical Fluids Induced by Shock and
Expansion Waves", ETH Zurich Institute of Fluid Dynamics, August 2003.

[10] Zainal Ahmad and Jie Zhang, "A Nonlinear Model Predictive Control Strategy
Using Multiple Neural Network Models", Springer-Verlag Berlin Heidelberg,
2006.

[11] Fuchen Sun, Yuehui Chen and Ajith Abraham, "Special Issue on Intelligent
Control and Robotics", Science Direct, April 2007.

[12] Guomin Xue, "Study on Spiral Tube Compound Gas-Liquid Separator with
Fuzzy PID Control".

[13] "Ideal Gas Law", 3 February 2009, http://en.wikipedia.org/wiki/Ideal_gas_law

[14] Twister BV, "Twister Supersonic Separator", 2009,
http://twisterbv.com/products-services/twister-supersonic-separator/

[15] Karl J. Astrom and Tore Hagglund, Advanced PID Control. Lund University: ISA Society, 2006.

[16] Dan Hammerstrom, "Neural Networks at Work", IEEE Spectrum, June 1993.

[17] Kenji Iwasa, Noboru Morizumi and Sigeru Omatu, "Pressure Control in a Plant Generating Chloride by Neural Network PID Control", University of Osaka Prefecture, 1993.

[18] A. R. Mirzai and J. R. Leigh, "An Overview of the Applications of Neural Networks in Process Engineering", Polytechnic of Central London, May 1992.

[19] Howard Demuth and Mark Beale, *Neural Network Toolbox for Use With Matlab*, The MathWorks Inc., Version 3, January 1998.

APPENDICES

APPENDIX A
ISENTROPIC COMPRESSIBLE FLOW TABLE

Table B.1
Isentropic Flow of a Perfect Gas, $k = 1.4$

Ma	p/p_0	ρ/ρ_0	T/T_0	A/A^*	Ma	p/p_0	ρ/ρ_0	T/T_0	A/A^*
0.0	1.0	1.0	1.0	∞	0.74	0.6951	0.7712	0.9013	1.0681
0.02	0.9997	0.9998	0.9999	28.9421	0.76	0.6821	0.7609	0.8964	1.0570
0.04	0.9989	0.9992	0.9997	14.4815	0.78	0.6690	0.7505	0.8915	1.0471
0.06	0.9975	0.9982	0.9993	9.6659	0.8	0.6560	0.7400	0.8865	1.0382
0.08	0.9955	0.9968	0.9987	7.2616	0.82	0.6430	0.7295	0.8815	1.0305
0.1	0.9930	0.9950	0.9980	5.8218	0.84	0.6300	0.7189	0.8763	1.0237
0.12	0.9900	0.9928	0.9971	4.8643	0.86	0.6170	0.7083	0.8711	1.0179
0.14	0.9864	0.9903	0.9961	4.1824	0.88	0.6041	0.6977	0.8659	1.0129
0.16	0.9823	0.9873	0.9949	3.6727	0.9	0.5913	0.6870	0.8606	1.0089
0.18	0.9776	0.9840	0.9936	3.2779	0.92	0.5785	0.6764	0.8552	1.0056
0.2	0.9725	0.9803	0.9921	2.9635	0.94	0.5658	0.6658	0.8498	1.0031
0.22	0.9668	0.9762	0.9904	2.7076	0.96	0.5532	0.6551	0.8444	1.0014
0.24	0.9607	0.9718	0.9886	2.4956	0.98	0.5407	0.6445	0.8389	1.0003
0.26	0.9541	0.9670	0.9867	2.3173	1.0	0.5283	0.6339	0.8333	1.0000
0.28	0.9470	0.9619	0.9846	2.1656	1.02	0.5160	0.6234	0.8278	1.0003
0.3	0.9395	0.9564	0.9823	2.0351	1.04	0.5039	0.6129	0.8222	1.0013
0.32	0.9315	0.9506	0.9799	1.9219	1.06	0.4919	0.6024	0.8165	1.0029
0.34	0.9231	0.9445	0.9774	1.8229	1.08	0.4800	0.5920	0.8108	1.0051
0.36	0.9143	0.9380	0.9747	1.7358	1.1	0.4684	0.5817	0.8052	1.0079
0.38	0.9052	0.9313	0.9719	1.6587	1.12	0.4568	0.5714	0.7994	1.0113
0.4	0.8956	0.9243	0.9690	1.5901	1.14	0.4455	0.5612	0.7937	1.0153
0.42	0.8857	0.9170	0.9659	1.5289	1.16	0.4343	0.5511	0.7879	1.0198
0.44	0.8755	0.9094	0.9627	1.4740	1.18	0.4232	0.5411	0.7822	1.0248
0.46	0.8650	0.9016	0.9594	1.4246	1.2	0.4124	0.5311	0.7764	1.0304
0.48	0.8541	0.8935	0.9559	1.3801	1.22	0.4017	0.5213	0.7706	1.0366
0.5	0.8430	0.8852	0.9524	1.3398	1.24	0.3912	0.5115	0.7648	1.0432
0.52	0.8317	0.8766	0.9487	1.3034	1.26	0.3809	0.5019	0.7590	1.0504
0.54	0.8201	0.8679	0.9449	1.2703	1.28	0.3708	0.4923	0.7532	1.0581
0.56	0.8082	0.8589	0.9410	1.2403	1.3	0.3609	0.4829	0.7474	1.0663
0.58	0.7962	0.8498	0.9370	1.2130	1.32	0.3512	0.4736	0.7416	1.0750
0.6	0.7840	0.8405	0.9328	1.1882	1.34	0.3417	0.4644	0.7358	1.0842
0.62	0.7716	0.8310	0.9286	1.1656	1.36	0.3323	0.4553	0.7300	1.0940
0.64	0.7591	0.8213	0.9243	1.1451	1.38	0.3232	0.4463	0.7242	1.1042
0.66	0.7465	0.8115	0.9199	1.1265	1.4	0.3142	0.4374	0.7184	1.1149
0.68	0.7338	0.8016	0.9153	1.1097	1.42	0.3055	0.4287	0.7126	1.1262
0.7	0.7209	0.7916	0.9107	1.0944	1.44	0.2969	0.4201	0.7069	1.1379
0.72	0.7080	0.7814	0.9061	1.0806	1.46	0.2886	0.4116	0.7011	1.1501

Table B.1 (*Cont.*)
Isentropic Flow of
a Perfect Gas,
$k = 1.4$

Ma	p/p_0	ρ/ρ_0	T/T_0	A/A^*	Ma	p/p_0	ρ/ρ_0	T/T_0	A/A^*
1.48	0.2804	0.4032	0.6954	1.1629	2.56	0.0533	0.1232	0.4328	2.7891
1.5	0.2724	0.3950	0.6897	1.1762	2.58	0.0517	0.1205	0.4289	2.8420
1.52	0.2646	0.3869	0.6840	1.1899	2.6	0.0501	0.1179	0.4252	2.8960
1.54	0.2570	0.3789	0.6783	1.2042	2.62	0.0486	0.1153	0.4214	2.9511
1.56	0.2496	0.3710	0.6726	1.2190	2.64	0.0471	0.1128	0.4177	3.0073
1.58	0.2423	0.3633	0.6670	1.2344	2.66	0.0457	0.1103	0.4141	3.0647
1.6	0.2353	0.3557	0.6614	1.2502	2.68	0.0443	0.1079	0.4104	3.1233
1.62	0.2284	0.3483	0.6558	1.2666	2.7	0.0430	0.1056	0.4068	3.1830
1.64	0.2217	0.3409	0.6502	1.2836	2.72	0.0417	0.1033	0.4033	3.2440
1.66	0.2151	0.3337	0.6447	1.3010	2.74	0.0404	0.1010	0.3998	3.3061
1.68	0.2088	0.3266	0.6392	1.3190	2.76	0.0392	0.0989	0.3963	3.3695
1.7	0.2026	0.3197	0.6337	1.3376	2.78	0.0380	0.0967	0.3928	3.4342
1.72	0.1966	0.3129	0.6283	1.3567	2.8	0.0368	0.0946	0.3894	3.5001
1.74	0.1907	0.3062	0.6229	1.3764	2.82	0.0357	0.0926	0.3860	3.5674
1.76	0.1850	0.2996	0.6175	1.3967	2.84	0.0347	0.0906	0.3827	3.6359
1.78	0.1794	0.2931	0.6121	1.4175	2.86	0.0336	0.0886	0.3794	3.7058
1.8	0.1740	0.2868	0.6068	1.4390	2.88	0.0326	0.0867	0.3761	3.7771
1.82	0.1688	0.2806	0.6015	1.4610	2.9	0.0317	0.0849	0.3729	3.8498
1.84	0.1637	0.2745	0.5963	1.4836	2.92	0.0307	0.0831	0.3696	3.9238
1.86	0.1587	0.2686	0.5910	1.5069	2.94	0.0298	0.0813	0.3665	3.9993
1.88	0.1539	0.2627	0.5859	1.5308	2.96	0.0289	0.0796	0.3633	4.0763
1.9	0.1492	0.2570	0.5807	1.5553	2.98	0.0281	0.0779	0.3602	4.1547
1.92	0.1447	0.2514	0.5756	1.5804	3.0	0.0272	0.0762	0.3571	4.2346
1.94	0.1403	0.2459	0.5705	1.6062	3.02	0.0264	0.0746	0.3541	4.3160
1.96	0.1360	0.2405	0.5655	1.6326	3.04	0.0256	0.0730	0.3511	4.3990
1.98	0.1318	0.2352	0.5605	1.6597	3.06	0.0249	0.0715	0.3481	4.4835
2.0	0.1278	0.2300	0.5556	1.6875	3.08	0.0242	0.0700	0.3452	4.5696
2.02	0.1239	0.2250	0.5506	1.7160	3.1	0.0234	0.0685	0.3422	4.6573
2.04	0.1201	0.2200	0.5458	1.7451	3.12	0.0228	0.0671	0.3393	4.7467
2.06	0.1164	0.2152	0.5409	1.7750	3.14	0.0221	0.0657	0.3365	4.8377
2.08	0.1128	0.2104	0.5361	1.8056	3.16	0.0215	0.0643	0.3337	4.9304
2.1	0.1094	0.2058	0.5313	1.8369	3.18	0.0208	0.0630	0.3309	5.0248
2.12	0.1060	0.2013	0.5266	1.8690	3.2	0.0202	0.0617	0.3281	5.1210
2.14	0.1027	0.1968	0.5219	1.9018	3.22	0.0196	0.0604	0.3253	5.2189
2.16	0.0996	0.1925	0.5173	1.9354	3.24	0.0191	0.0591	0.3226	5.3186
2.18	0.0965	0.1882	0.5127	1.9698	3.26	0.0185	0.0579	0.3199	5.4201
2.2	0.0935	0.1841	0.5081	2.0050	3.28	0.0180	0.0567	0.3173	5.5234
2.22	0.0906	0.1800	0.5036	2.0409	3.3	0.0175	0.0555	0.3147	5.6286
2.24	0.0878	0.1760	0.4991	2.0777	3.32	0.0170	0.0544	0.3121	5.7358
2.26	0.0851	0.1721	0.4947	2.1153	3.34	0.0165	0.0533	0.3095	5.8448
2.28	0.0825	0.1683	0.4903	2.1538	3.36	0.0160	0.0522	0.3069	5.9558
2.3	0.0800	0.1646	0.4859	2.1931	3.38	0.0156	0.0511	0.3044	6.0687

APPENDIX B

UPSTREAM PRESSURE MATLAB FUNCTION

```matlab
clear all;
close all;
clc;

R0=0.025;
R=0.025;
A01=0;
A1=0;
A101=0;
i=1;
a=340.46;

for (R=0.025:0.0001:0.050)

        %Area Ratio
        R1(i,1)=R;                          %Radius
        A01(i,1)=pi*(R0^2);                 %Sonic throat (A*)
        A1(i,1)=pi*(R1(i,1).^2);            %Area (A)
        A101(i,1)=A1(i,1)./A01(i,1);        %A/A*

        %Supersonic Mach Number Profile
        if (1<=A101(i,1))&&(A101(i,1)<=2.9)
            Mu(i,1)        = 1+(1.2*((A101(i,1)-1)^0.5));
        else
            Mu(i,1)        = ((216*A101(i,1))-
(254*(A101(i,1)^(2/3))))^(1/5);
        end

        %Supersonic Velocity Profile
            Vsuper(i,1)    = Mu(i,1)*a;

        %Supersonic Pressure Profile
            P10super(i,1) = 1/((1+(0.2*(Mu(i,1)^2)))^3.5);

            i=i+1;

end


subplot (3,1,1)
plot (R1,Mu)
subplot (3,1,2)
plot (R1,Vsuper)
subplot (3,1,3)
plot (R1,P10super)
```

APPENDIX C

DOWNSTREAM PRESSURE MATLAB FUNCTION

```matlab
clear all;
close all;
clc;

%Define pressure ratio of control zone
P10super =
[0.043636818;0.043266872;0.042901763;0.042541401;0.042185698;0
.041834567;0.041487925;0.041145691;0.040807783;0.040474126;0.0
40144641];
Mu       =
[2.689687853;2.69522133;2.700731123;2.706217539;2.711680881;2.
717121443;2.722539514;2.727935376;2.733309306;2.738661576;2.74
3992452];
i=0;
j=0;

%Define inlet pressure in kPa
P=5066.25;

for (j=1:1:11)

    for (i=1:1:100)

        %upstream pressure
        P01(i,1) = P;
        P1(i,j) = P*P10super(j,1);

        %Pressure at PT1
        PT1(i,1) = P01(i,1)./((1+(0.2*(2.689687853^2)))^3.5);

        %downstream pressure
        P2(i,j) = P1(i,j)*0.41666*((2.8*(Mu(j,1)^2))-0.4);

        %downstream mach number
        Md(j,1) = (((((0.4*Mu(j,1)^2)+2)/((2.8*Mu(j,1)^2)-
0.4))^0.5);

        %downstream effective area
        A02(j,1) =
0.001963*(Md(j,1)/Mu(j,1))*(((2+(0.4*(Mu(j,1)^2)))/(2+(0.4*(Md
(j,1)^2))))^3);

        %downstream effective area ratio at PT2
        A202(j,1)= 0.00658993/A02(j,1);

        %Mach Number at PT2
        Md2(j,1) = (1+(0.27*(A202(j,1)^2)))/(1728*A202(j,1));

        %Pressure ratio at PT2
        PT202(j,1) = 1/((1+(0.2*(Md2(j,1)^2)))^3.5);
```

```matlab
        %Pressure at PT2
        PT2(i,j)   = PT202(j,1)*P02(i,1);

        %Valve Area
        Av(j,1)     =
(((1+(0.2*Md(j,1)^2))^3)/(1.728*Md(j,1)))*A02(j,1);

        %Valve Percentage (100%=0.0092857m^2)
        VP(j,1)     = (Av(j,1)/0.0092857)*100;



        P = P+101.325;



    end

end

```

APPENDIX D

NEURAL NETWORK SYSTEM MATLAB FUNCTION

```
clear all;
close all;
clc;

%Load data
x = load ('input.txt')';
y = load ('output.txt')';

%Divide data for training and validation
train_data = 550;
validation_data = 550;
numofvar=size(x,1);
numofout=size(y,1);

%Load data into matrix
for m=1:numofvar
    for n=1:train_data
    x_t(m,n)=x(m,n);
    end
end

for m=1:numofvar
    for n=1:validation_data
    x_v(m,n)=x(m,n+train_data);
    end
end

for m=1:numofout
    for n=1:train_data
    y_t(m,n)=y(m,n);
    end
end

for m=1:numofout
    for n=1:validation_data
    y_v(m,n)=y(m,n+train_data);
    end
end

%Normalize data
[x_t1,x_s1] = mapminmax(x_t);
[y_t1,y_s1] = mapminmax(y_t);
[x_v1,x_s2] = mapminmax(x_v);
[y_v1,y_s2] = mapminmax(y_v);
t = minmax(x_t1);

%Initialize number of neurons
neuron_1 =10;
neuron_2 =1;
```

```matlab
%Initialize system variables and parameters
net=newff(x_t1,y_t1,neuron_1,{'purelin','purelin'},'trainlm');
net.trainParam.show = 50;
net.trainParam.lr = 0.1;
net.trainParam.epochs = 10000;
net.trainParam.goal = 0.001;
net=init(net);

%Initialize weight
for m=1:neuron_1
    for n=1:numofvar
    w_1(m,n)=3;
    end
end
net.IW{1,1}=w_1;


for m=1:numofout
    for n=1:neuron_1
    w_2(m,n)=0;
    end
end
net.LW{2,1}=w_2;



%Initialize bias
for m=1:neuron_1
    b_1(m,1)=0;
end
net.b{1}=b_1;


for m=1:numofout
    b_2(m,1)=0;
end
net.b{2}=b_2;

%Train network
[net,tr]=train(net,x_t1,y_t1);


%Denormalize data for analysis
xtest_t = mapminmax('apply',x_t,x_s1);
ytrain = sim(net,xtest_t);
ytrain1 = mapminmax('reverse',ytrain,y_s1);
etrain=y_t-ytrain1;
```

```matlab
%Analysis of results
xtest_v = mapminmax('apply', x_v, x_s1);
yvalid=sim(net,xtest_v);
yvalid1 = mapminmax('reverse',yvalid,y_s1);
evalid=y_v-yvalid1;

subplot(2,2,1);
plot (yvalid1,'r');
hold on;
plot (y_v,'b');
xlabel('No of Data');
ylabel('Valve Opening (%)');
title('Output of NN model (Validation Data)');
legend('Predicted','Actual');
grid on;

subplot(2,2,2);
plot(evalid,'*r');
xlabel('No of data');
ylabel('Error Valve Opening (%))');
title('Error between Actual Valve Opening and Predicted Valve
Opening (Validation Data)');
grid on;

subplot(2,2,3);
plot (ytrain1,'r');
hold on;
plot (y_t,'b');
xlabel('No of Data');
ylabel('Valve Opening (%)');
title('Output of NN model (Training Data)');
legend('Predicted','Actual');
grid on;

subplot(2,2,4);
plot(etrain,'*r');
xlabel('No of Data');
ylabel('Error Valve Opening (%))');
title('Error between Actual Valve Opening and Predicted Valve
Opening (Training Data)');
grid on;


fit_valid = (1-norm(evalid)/norm(y_v-mean(y_v)))*100
rmse_valid = sqrt(mse(evalid))
index_valid = (sum((evalid).^2)/sum((y_v-mean(y_v)).^2))*100
correlation = corrcoef (y_v,yvalid1)
actualValida_predictedValid = [y_v' yvalid1']


fit_train = (1-norm(etrain)/norm(y_t-mean(y_t)))*100
rmse_train = sqrt(mse(etrain))
index_train = (sum((etrain).^2)/sum((y_t-mean(y_t)).^2))*100
correlation = corrcoef (y_t,ytrain1)
actualTrain_predictedTrain = [y_t' ytrain1']
```

APPENDIX E

TABULATED DATA FROM CFD ANALYSIS

Input			Output
P0	PT1	PT2	VP %
106391.25	4642.57560	19126.69	68.03825
112673.40	4916.70864	34046.93	69.09551
108316.42	4726.58411	24074.91	68.39023
113990.62	4974.18815	18146.72	67.68671
111356.17	4859.22913	12825.34	67.3356
106897.87	4664.68310	15157.85	67.68671
115713.15	5049.35365	18872.59	67.68671
106391.25	4642.57560	6463.745	66.98492
115713.15	5049.35365	39320.35	69.44882
112876.05	4925.55164	30073.37	68.74265
106391.25	4642.57560	35480.15	69.44882
107607.15	4695.63361	43933.86	70.15678
109633.65	4784.06362	44761.24	70.15678
109228.35	4766.37762	44595.77	70.15678
115510.50	5040.51065	22952.03	68.03825
114294.60	4987.45265	5541.216	66.63467
112673.40	4916.70864	4848.564	66.63467
115206.52	5027.24615	43091.96	69.80257
114294.60	4987.45265	26571.25	68.39023
106796.55	4660.26160	2337.701	66.63467
110444.25	4819.43562	12439.29	67.3356
113180.02	4938.81614	42260.87	69.80257
110444.25	4819.43562	16652.28	67.68671
111254.85	4854.80763	29399.46	68.74265
116321.10	5075.88266	14927.15	67.3356
113787.97	4965.34514	46457.37	70.15678
106999.20	4669.10461	35730.6	69.44882
115307.85	5031.66765	39153.39	69.44882
114395.92	4991.87415	14112.16	67.3356
115003.87	5018.40315	46953.8	70.15678
108519.07	4735.42711	7368.669	66.98492
115713.15	5049.35365	6147.287	66.63467
115409.17	5036.08915	31126.36	68.74265
112673.40	4916.70864	21761.93	68.03825
107607.15	4695.63361	39975.38	69.80257
112369.42	4903.44414	17463.55	67.68671

106897.87	4664.68310	35688.86	69.44882
113382.67	4947.65914	34340.44	69.09551
111457.50	4863.65063	33543.77	69.09551
111356.17	4859.22913	21209.38	68.03825
107911.12	4708.89811	15584.83	67.68671
113484.00	4952.08064	42385.54	69.80257
107505.82	4691.21211	35939.3	69.44882
111457.50	4863.65063	8618.326	66.98492
108316.42	4726.58411	11538.51	67.3356
113990.62	4974.18815	9695.617	66.98492
107404.50	4686.79061	23694.11	68.39023
114294.60	4987.45265	14069.27	67.3356
106391.25	4642.57560	27377.72	68.74265
110646.90	4828.27863	20911.85	68.03825
114294.60	4987.45265	30663.04	68.74265
109734.97	4788.48512	40848.02	69.80257
116118.45	5067.03966	43465.95	69.80257
110545.57	4823.85713	45133.56	70.15678
110545.57	4823.85713	41180.46	69.80257
115307.85	5031.66765	10255.81	66.98492
110950.87	4841.54313	21039.36	68.03825
106695.22	4655.84010	2294.41	66.63467
113686.65	4960.92364	38485.53	69.44882
112774.72	4921.13014	38109.86	69.44882
108924.37	4753.11312	16011.81	67.68671
115003.87	5018.40315	18573.7	67.68671
114598.57	5000.71715	30789.4	68.74265
113484.00	4952.08064	46333.27	70.15678
111964.12	4885.75813	29694.29	68.74265
110849.55	4837.12163	41305.12	69.80257
114598.57	5000.71715	42842.64	69.80257
113585.32	4956.50214	13769.01	67.3356
108620.40	4739.84861	15883.71	67.68671
108215.10	4722.16261	36231.49	69.44882
115307.85	5031.66765	31084.24	68.74265
115611.82	5044.93215	39278.61	69.44882
111153.52	4850.38613	37441.99	69.44882
109734.97	4788.48512	12139.03	67.3356
107505.82	4691.21211	2640.736	66.63467
107100.52	4673.52611	43727.02	70.15678
113889.30	4969.76664	46498.74	70.15678
112369.42	4903.44414	45878.21	70.15678
107708.47	4700.05511	40016.93	69.80257
109025.70	4757.53462	40557.14	69.80257
112876.05	4925.55164	4935.146	66.63467

107607.15	4695.63361	31950.45	69.09551
106897.87	4664.68310	23482.55	68.39023
112673.40	4916.70864	29989.13	68.74265
106999.20	4669.10461	23524.86	68.39023
109734.97	4788.48512	7885.769	66.98492
106897.87	4664.68310	19339.21	68.03825
110140.27	4806.17112	37024.58	69.44882
113585.32	4956.50214	42427.09	69.80257
108012.45	4713.31961	2857.19	66.63467
112876.05	4925.55164	38151.6	69.44882
110444.25	4819.43562	20826.84	68.03825
107911.12	4708.89811	40100.04	69.80257
109127.02	4761.95612	7627.219	66.98492
109431.00	4775.22062	16225.3	67.68671
112369.42	4903.44414	33921.14	69.09551
115915.80	5058.19666	23122.05	68.03825
112166.77	4894.60113	29778.53	68.74265
110950.87	4841.54313	8402.868	66.98492
113889.30	4969.76664	34550.09	69.09551
114699.90	5005.13865	18445.6	67.68671
111254.85	4854.80763	25301.92	68.39023
111052.20	4845.96463	21081.87	68.03825
110748.22	4832.70013	4026.04	66.63467
109127.02	4761.95612	3333.388	66.63467
115915.80	5058.19666	43382.84	69.80257
114598.57	5000.71715	26698.18	68.39023
107809.80	4704.47661	44016.6	70.15678
113585.32	4956.50214	34424.3	69.09551
111052.20	4845.96463	25217.3	68.39023
113484.00	4952.08064	34382.37	69.09551
116219.77	5071.46116	43507.51	69.80257
107201.85	4677.94761	11066.68	67.3356
109734.97	4788.48512	36857.61	69.44882
110038.95	4801.74962	20656.83	68.03825
115409.17	5036.08915	27036.67	68.39023
112369.42	4903.44414	25767.34	68.39023
107607.15	4695.63361	11238.26	67.3356
111052.20	4845.96463	8445.96	66.98492
116219.77	5071.46116	10643.63	66.98492
107708.47	4700.05511	27925.27	68.74265
107708.47	4700.05511	31992.38	69.09551
110241.60	4810.59262	33040.62	69.09551
112977.37	4929.97314	21889.44	68.03825
108215.10	4722.16261	32202.02	69.09551
113484.00	4952.08064	30326.09	68.74265

111862.80	4881.33663	37734.18	69.44882
114294.60	4987.45265	38735.98	69.44882
113281.35	4943.23764	9393.976	66.98492
113990.62	4974.18815	22314.48	68.03825
113281.35	4943.23764	26148.14	68.39023
115814.47	5053.77516	6190.577	66.63467
106796.55	4660.26160	43602.91	70.15678
113889.30	4969.76664	13897.69	67.3356
109836.30	4792.90662	3636.423	66.63467
115915.80	5058.19666	10514.36	66.98492
109431.00	4775.22062	3463.26	66.63467
108316.42	4726.58411	7282.486	66.98492
108316.42	4726.58411	40266.26	69.80257
111356.17	4859.22913	25344.23	68.39023
107404.50	4686.79061	11152.47	67.3356
110849.55	4837.12163	20996.86	68.03825
109228.35	4766.37762	28557.06	68.74265
109329.67	4770.79912	32663.25	69.09551
106999.20	4669.10461	19381.72	68.03825
115206.52	5027.24615	39111.65	69.44882
109836.30	4792.90662	20571.82	68.03825
109127.02	4761.95612	11881.67	67.3356
114091.95	4978.60965	30578.8	68.74265
107201.85	4677.94761	43768.39	70.15678
112876.05	4925.55164	21846.93	68.03825
109734.97	4788.48512	32830.97	69.09551
114699.90	5005.13865	42884.19	69.80257
114598.57	5000.71715	34843.6	69.09551
107404.50	4686.79061	27798.91	68.74265
116321.10	5075.88266	39570.8	69.44882
110646.90	4828.27863	37233.29	69.44882
113686.65	4960.92364	42468.65	69.80257
110342.92	4815.01412	29020.38	68.74265
115611.82	5044.93215	18829.89	67.68671
109228.35	4766.37762	40640.25	69.80257
111862.80	4881.33663	25555.79	68.39023
108823.05	4748.69162	11752.99	67.3356
114193.27	4983.03115	5497.925	66.63467
110342.92	4815.01412	8144.318	66.98492
111356.17	4859.22913	45464.52	70.15678
107100.52	4673.52611	23567.17	68.39023
110748.22	4832.70013	16780.38	67.68671
106492.57	4646.99710	2207.828	66.63467
114294.60	4987.45265	46664.22	70.15678
111964.12	4885.75813	8833.784	66.98492

111153.52	4850.38613	4199.203	66.63467
111457.50	4863.65063	12868.23	67.3356
107708.47	4700.05511	43975.23	70.15678
109734.97	4788.48512	3593.132	66.63467
106695.22	4655.84010	23397.93	68.39023
109127.02	4761.95612	24413.39	68.39023
114193.27	4983.03115	34675.88	69.09551
112470.75	4907.86564	33963.07	69.09551
109937.62	4797.32812	20614.33	68.03825
109431.00	4775.22062	32705.18	69.09551
113686.65	4960.92364	5281.472	66.63467
115915.80	5058.19666	35388.68	69.09551
109532.32	4779.64212	3506.551	66.63467
112065.45	4890.17963	8876.876	66.98492
107708.47	4700.05511	15499.43	67.68671
114395.92	4991.87415	30705.16	68.74265
113990.62	4974.18815	30536.68	68.74265
109937.62	4797.32812	16438.79	67.68671
115003.87	5018.40315	43008.85	69.80257
113382.67	4947.65914	42343.98	69.80257
107708.47	4700.05511	23821.04	68.39023
107100.52	4673.52611	27672.55	68.74265
114497.25	4996.29565	30747.28	68.74265
115814.47	5053.77516	10471.27	66.98492
107809.80	4704.47661	7067.028	66.98492
114395.92	4991.87415	38777.72	69.44882
111862.80	4881.33663	33711.49	69.09551
112166.77	4894.60113	4632.11	66.63467
115510.50	5040.51065	43216.63	69.80257
112977.37	4929.97314	46126.42	70.15678
113078.70	4934.39464	30157.61	68.74265
108924.37	4753.11312	7541.035	66.98492
108012.45	4713.31961	19806.75	68.03825
113180.02	4938.81614	34256.58	69.09551
112774.72	4921.13014	9178.517	66.98492
113484.00	4952.08064	5194.89	66.63467
107505.82	4691.21211	39933.83	69.80257
109431.00	4775.22062	7756.494	66.98492
107505.82	4691.21211	31908.52	69.09551
107607.15	4695.63361	23778.73	68.39023
109734.97	4788.48512	24667.26	68.39023
110342.92	4815.01412	41097.35	69.80257
111862.80	4881.33663	13039.81	67.3356
112065.45	4890.17963	4588.82	66.63467
108417.75	4731.00561	28220.11	68.74265

108417.75	4731.00561	15798.32	67.68671
108519.07	4735.42711	3073.643	66.63467
108721.72	4744.27012	11710.09	67.3356
109633.65	4784.06362	28725.54	68.74265
111862.80	4881.33663	8790.693	66.98492
108823.05	4748.69162	3203.516	66.63467
110545.57	4823.85713	25005.75	68.39023
113787.97	4965.34514	18061.32	67.68671
114193.27	4983.03115	22399.48	68.03825
111254.85	4854.80763	41471.34	69.80257
109329.67	4770.79912	28599.18	68.74265
108316.42	4726.58411	36273.24	69.44882
109836.30	4792.90662	16396.09	67.68671
112774.72	4921.13014	4891.855	66.63467
109937.62	4797.32812	12224.82	67.3356
112268.10	4899.02264	13211.39	67.3356
115206.52	5027.24615	5930.833	66.63467
110342.92	4815.01412	37108.06	69.44882
106593.90	4651.41860	19211.7	68.03825
108823.05	4748.69162	7497.944	66.98492
110140.27	4806.17112	16524.19	67.68671
108316.42	4726.58411	15755.62	67.68671
113281.35	4943.23764	42302.43	69.80257
108620.40	4739.84861	7411.761	66.98492
114193.27	4983.03115	30620.92	68.74265
114497.25	4996.29565	14155.06	67.3356
115003.87	5018.40315	35011.31	69.09551
110849.55	4837.12163	16823.07	67.68671
113889.30	4969.76664	38569.01	69.44882
108316.42	4726.58411	19934.27	68.03825
110038.95	4801.74962	16481.49	67.68671
109532.32	4779.64212	40764.91	69.80257
115611.82	5044.93215	27121.29	68.39023
111558.82	4868.07213	29525.81	68.74265
106999.20	4669.10461	39726.05	69.80257
111558.82	4868.07213	33585.7	69.09551
113787.97	4965.34514	5324.762	66.63467
111964.12	4885.75813	25598.1	68.39023
107708.47	4700.05511	19679.24	68.03825
111660.15	4872.49363	37650.7	69.44882
110950.87	4841.54313	25174.99	68.39023
111254.85	4854.80763	4242.494	66.63467
109836.30	4792.90662	36899.36	69.44882
116219.77	5071.46116	39529.06	69.44882
113787.97	4965.34514	34508.16	69.09551

108823.05	4748.69162	32453.6	69.09551
114801.22	5009.56015	30873.64	68.74265
108620.40	4739.84861	40390.92	69.80257
108012.45	4713.31961	44099.34	70.15678
106492.57	4646.99710	35521.89	69.44882
107303.17	4682.36911	39850.72	69.80257
111052.20	4845.96463	4155.912	66.63467
109228.35	4766.37762	32621.32	69.09551
109532.32	4779.64212	12053.24	67.3356
109937.62	4797.32812	32914.83	69.09551
111558.82	4868.07213	4372.366	66.63467
109228.35	4766.37762	7670.31	66.98492
114902.55	5013.98165	22697.01	68.03825
113382.67	4947.65914	30283.97	68.74265
116422.42	5080.30416	19171.47	67.68671
110241.60	4810.59262	3809.586	66.63467
110849.55	4837.12163	33292.2	69.09551
106999.20	4669.10461	15200.54	67.68671
112673.40	4916.70864	25894.27	68.39023
114193.27	4983.03115	46622.85	70.15678
112572.07	4912.28714	45960.94	70.15678
113078.70	4934.39464	38235.08	69.44882
110038.95	4801.74962	24794.19	68.39023
107911.12	4708.89811	11366.94	67.3356
108519.07	4735.42711	36356.72	69.44882
112876.05	4925.55164	13468.75	67.3356
113281.35	4943.23764	46250.53	70.15678
115611.82	5044.93215	31210.6	68.74265
111558.82	4868.07213	45547.25	70.15678
111558.82	4868.07213	41596	69.80257
110748.22	4832.70013	41263.57	69.80257
110950.87	4841.54313	37358.51	69.44882
116219.77	5071.46116	47450.23	70.15678
114497.25	4996.29565	18360.21	67.68671
109633.65	4784.06362	32789.04	69.09551
108823.05	4748.69162	24286.46	68.39023
107201.85	4677.94761	35814.08	69.44882
110038.95	4801.74962	40972.69	69.80257
109937.62	4797.32812	7971.952	66.98492
108823.05	4748.69162	28388.59	68.74265
106593.90	4651.41860	31531.15	69.09551
116422.42	5080.30416	39612.54	69.44882
115206.52	5027.24615	26952.05	68.39023
114193.27	4983.03115	9781.8	66.98492
111761.47	4876.91513	4458.947	66.63467

113382.67	4947.65914	22059.45	68.03825
115105.20	5022.82465	10169.63	66.98492
116422.42	5080.30416	43590.62	69.80257
115105.20	5022.82465	39069.91	69.44882
108215.10	4722.16261	7239.394	66.98492
114699.90	5005.13865	14240.84	67.3356
107404.50	4686.79061	43851.13	70.15678
107911.12	4708.89811	36106.27	69.44882
112673.40	4916.70864	17591.64	67.68671
107100.52	4673.52611	15243.24	67.68671
109127.02	4761.95612	44554.4	70.15678
112065.45	4890.17963	29736.41	68.74265
114395.92	4991.87415	46705.59	70.15678
109532.32	4779.64212	20444.31	68.03825
110140.27	4806.17112	24836.5	68.39023
107809.80	4704.47661	19721.75	68.03825
113889.30	4969.76664	5368.053	66.63467
110950.87	4841.54313	29273.1	68.74265
115206.52	5027.24615	22824.52	68.03825
114497.25	4996.29565	5627.798	66.63467
110444.25	4819.43562	8187.41	66.98492
116219.77	5071.46116	19086.08	67.68671
114902.55	5013.98165	30915.76	68.74265
111964.12	4885.75813	4545.529	66.63467
116017.12	5062.61816	39445.58	69.44882
108924.37	4753.11312	11795.88	67.3356
113686.65	4960.92364	22186.96	68.03825
115713.15	5049.35365	14669.78	67.3356
114497.25	4996.29565	26655.87	68.39023
110849.55	4837.12163	37316.77	69.44882
116219.77	5071.46116	27375.16	68.39023
112369.42	4903.44414	9006.151	66.98492
109329.67	4770.79912	40681.81	69.80257
109431.00	4775.22062	24540.33	68.39023
106593.90	4651.41860	10809.32	67.3356
111660.15	4872.49363	21336.89	68.03825
115307.85	5031.66765	26994.36	68.39023
107404.50	4686.79061	6894.661	66.98492
107607.15	4695.63361	35981.05	69.44882
115510.50	5040.51065	10341.99	66.98492
111153.52	4850.38613	16951.17	67.68671
113585.32	4956.50214	17975.92	67.68671
112774.72	4921.13014	17634.34	67.68671
115003.87	5018.40315	30957.88	68.74265
106897.87	4664.68310	43644.28	70.15678

112774.72	4921.13014	21804.43	68.03825
108924.37	4753.11312	32495.53	69.09551
112572.07	4912.28714	9092.334	66.98492
111964.12	4885.75813	21464.4	68.03825
108417.75	4731.00561	11581.41	67.3356
108924.37	4753.11312	24328.77	68.39023
116321.10	5075.88266	6407.031	66.63467
112065.45	4890.17963	13125.6	67.3356
113990.62	4974.18815	26444.32	68.39023
111052.20	4845.96463	41388.23	69.80257
106391.25	4642.57560	31447.29	69.09551
114091.95	4978.60965	13983.48	67.3356
114801.22	5009.56015	22654.51	68.03825
116219.77	5071.46116	6363.74	66.63467
110444.25	4819.43562	41138.9	69.80257
108113.77	4717.74111	36189.75	69.44882
110140.27	4806.17112	12310.61	67.3356
114801.22	5009.56015	14283.74	67.3356
113585.32	4956.50214	30368.2	68.74265
109025.70	4757.53462	44513.03	70.15678
111558.82	4868.07213	17121.96	67.68671
108012.45	4713.31961	36148.01	69.44882
109937.62	4797.32812	36941.1	69.44882
108519.07	4735.42711	44306.19	70.15678
110241.60	4810.59262	8101.227	66.98492
106391.25	4642.57560	14944.36	67.68671
115915.80	5058.19666	27248.22	68.39023
108721.72	4744.27012	24244.15	68.39023
108721.72	4744.27012	36440.2	69.44882
112470.75	4907.86564	41969.99	69.80257
113180.02	4938.81614	17805.13	67.68671
112977.37	4929.97314	26021.21	68.39023
110140.27	4806.17112	3766.295	66.63467
114699.90	5005.13865	5714.379	66.63467
110646.90	4828.27863	29146.74	68.74265
114395.92	4991.87415	5584.507	66.63467
110849.55	4837.12163	12610.87	67.3356
106999.20	4669.10461	43685.65	70.15678
113787.97	4965.34514	38527.27	69.44882
113585.32	4956.50214	9523.251	66.98492
115814.47	5053.77516	39362.1	69.44882
106796.55	4660.26160	6636.111	66.98492
112369.42	4903.44414	4718.692	66.63467
111457.50	4863.65063	25386.54	68.39023
110444.25	4819.43562	33124.48	69.09551

106695.22	4655.84010	10852.21	67.3356
113585.32	4956.50214	38443.79	69.44882
111761.47	4876.91513	41679.11	69.80257
110950.87	4841.54313	41346.68	69.80257
109532.32	4779.64212	24582.64	68.39023
116017.12	5062.61816	14798.47	67.3356
109836.30	4792.90662	40889.58	69.80257
112268.10	4899.02264	21591.91	68.03825
109734.97	4788.48512	44802.61	70.15678
107404.50	4686.79061	31866.59	69.09551
110241.60	4810.59262	28978.26	68.74265
116017.12	5062.61816	43424.4	69.80257
115105.20	5022.82465	14412.42	67.3356
111558.82	4868.07213	8661.418	66.98492
112977.37	4929.97314	34172.72	69.09551
107607.15	4695.63361	2684.027	66.63467
108924.37	4753.11312	44471.66	70.15678
111964.12	4885.75813	45712.73	70.15678
112977.37	4929.97314	30115.49	68.74265
115814.47	5053.77516	31294.84	68.74265
112673.40	4916.70864	9135.426	66.98492
108620.40	4739.84861	20061.78	68.03825
110241.60	4810.59262	12353.5	67.3356
112065.45	4890.17963	25640.41	68.39023
107809.80	4704.47661	27967.39	68.74265
110950.87	4841.54313	33334.13	69.09551
108519.07	4735.42711	20019.27	68.03825
108620.40	4739.84861	44347.55	70.15678
112166.77	4894.60113	41845.33	69.80257
115003.87	5018.40315	22739.51	68.03825
108519.07	4735.42711	28262.23	68.74265
107607.15	4695.63361	15456.73	67.68671
110140.27	4806.17112	20699.33	68.03825
113889.30	4969.76664	26402	68.39023
111052.20	4845.96463	37400.25	69.44882
109734.97	4788.48512	28767.66	68.74265
114193.27	4983.03115	38694.23	69.44882
111660.15	4872.49363	33627.63	69.09551
107303.17	4682.36911	11109.57	67.3356
108215.10	4722.16261	28135.87	68.74265
110646.90	4828.27863	3982.749	66.63467
114497.25	4996.29565	46746.96	70.15678
107607.15	4695.63361	6980.844	66.98492
110646.90	4828.27863	12525.08	67.3356
111660.15	4872.49363	41637.56	69.80257

113686.65	4960.92364	9566.342	66.98492
112369.42	4903.44414	29862.77	68.74265
115105.20	5022.82465	18616.4	67.68671
109937.62	4797.32812	40931.13	69.80257
113990.62	4974.18815	5411.344	66.63467
107201.85	4677.94761	23609.49	68.39023
109633.65	4784.06362	16310.7	67.68671
113281.35	4943.23764	17847.83	67.68671
115915.80	5058.19666	47326.12	70.15678
112774.72	4921.13014	13425.86	67.3356
116017.12	5062.61816	23164.55	68.03825
112268.10	4899.02264	29820.65	68.74265
115409.17	5036.08915	6017.414	66.63467
112977.37	4929.97314	17719.74	67.68671
112369.42	4903.44414	37942.89	69.44882
113686.65	4960.92364	13811.9	67.3356
112065.45	4890.17963	37817.67	69.44882
106593.90	4651.41860	23355.62	68.39023
115409.17	5036.08915	22909.53	68.03825
114801.22	5009.56015	38944.68	69.44882
112673.40	4916.70864	13382.96	67.3356
115206.52	5027.24615	35095.17	69.09551
112774.72	4921.13014	25936.58	68.39023
114801.22	5009.56015	34927.46	69.09551
107404.50	4686.79061	15371.34	67.68671
115307.85	5031.66765	18701.79	67.68671
111356.17	4859.22913	29441.57	68.74265
115206.52	5027.24615	18659.1	67.68671
108012.45	4713.31961	11409.83	67.3356
107303.17	4682.36911	35855.82	69.44882
107100.52	4673.52611	19424.22	68.03825
112268.10	4899.02264	8963.059	66.98492
106999.20	4669.10461	10980.89	67.3356
109025.70	4757.53462	32537.46	69.09551
107303.17	4682.36911	27756.79	68.74265
106492.57	4646.99710	27419.84	68.74265
110950.87	4841.54313	16865.77	67.68671
112470.75	4907.86564	29904.89	68.74265
111964.12	4885.75813	17292.75	67.68671
113078.70	4934.39464	26063.52	68.39023
108417.75	4731.00561	19976.77	68.03825
112572.07	4912.28714	42011.55	69.80257
111761.47	4876.91513	37692.44	69.44882
109734.97	4788.48512	20529.32	68.03825
112065.45	4890.17963	17335.45	67.68671

106492.57	4646.99710	19169.2	68.03825
111862.80	4881.33663	41720.67	69.80257
109025.70	4757.53462	36565.43	69.44882
107303.17	4682.36911	31824.66	69.09551
111356.17	4859.22913	37525.48	69.44882
108519.07	4735.42711	32327.81	69.09551
110545.57	4823.85713	16694.98	67.68671
113889.30	4969.76664	30494.56	68.74265
113787.97	4965.34514	9609.434	66.98492
110849.55	4837.12163	4069.331	66.63467
106391.25	4642.57560	43437.44	70.15678
109025.70	4757.53462	20231.79	68.03825
116422.42	5080.30416	14970.04	67.3356
111254.85	4854.80763	21166.87	68.03825